Environ. Eng. Res. 2019; 24(3): 521-528
https://doi.org/10.4491/eer.2018.073

pISSN 1226-1025
eISSN 2005-968X

Assessment of gas production and electrochemical factors for fracturing flow-back fluid treatment in Guangyuan oilfield

Yang Liu[1,2], Wu Chen[1,2†], Shanhui Zhang[1,2], Dongpo Shi[1,2], Mijia Zhu[1,2†]

[1]*School of Chemistry and Environmental Engineering, Yangtze University, Jingzhou 434023, China*
[2]*State Key Laboratory of Petroleum Pollution Control, HSE Key Laboratory, CNPC Research Institute of Safety and Environmental Technology, Beijing 102206, China*

ABSTRACT

Electrochemical method was used for the fracturing flow-back fluid treatment in Guangyuan oilfield. After performing electrolysis, we found that the amount of H_2 gas produced by electrode was closely related to the combination mode of electrodes and electrode materials. Using an aluminium electrode resulted in a large H_2 production of each electrode combination, whereas inert anode and cathode materials resulted in low H_2 production. Then, the relationship between the gas production of H_2 and the treatment efficiency of fracturing flow-back fluid in Guangyuan oilfield was studied. Results showed that the turbidity removal and decolourisation rates of fracturing flow-back fluid were high when H_2 production was high. If the H_2 production of inert electrode was large, the energy consumption of this inert electrode was also high. However, energy consumption when an aluminium anode material was used was lower than that when the inert electrode was used, whereas the corresponding electrode combination production of H_2 was larger than that of the inert electrode combination. When the inert electrode was used as anode, the gas production type was mainly O_2, and Cl_2 was also produced and dissolved in water to form ClO^-. H_2 production at the cathode was reduced because ClO^- obtained electrons.

Keywords: Aluminium electrode, Electrolysis, Hydrogen evolution, H_2 production, Inert electrode

1. Introduction

Fracturing flow-back fluid is one of the main pollutants produced in oilfield exploitation [1-2]. The composition of flow-back fluid is extremely complex. Further treatment of all types of organic pollutants in waste fluid is necessary prior to its reuse or discharge. Electrochemical method is an effective way for processing fracturing flow-back fluid in oilfield [3] and involves electrocoagulation [4-6], electrolytic flotation [7-9], and electrochemical oxidation methods [10-13]. These electrochemical methods produce a considerable amount of gases, such as H_2, O_2 or Cl_2, in the electrode during the fracturing fluid treatment [14-15]. O_2, Cl_2 and other strong oxidising gases are often comprehensively involved in the reaction of degraded or oxidised organic compounds in wastewater, which cause a significant decrease in their electrolytic production. Therefore, these gases do not evidently harm the environment. However, H_2 produced by the cathode is difficult to consume in the electrolysis process and thus a major safety hazard during the electrochemical treatment of fracturing flow-back fluid. Research on electrochemical treatment of fracturing flow-back fluid in oilfield mainly focuses on treatment effect, and no systematic report on the study of H_2 electrode analysis is currently available. Therefore, the Guangyuan oilfield fracturing flow-back fluid was considered as the processing object in this study. The amount of H_2 produced and the effect of different electrodes and electrode combinations on the treatment of fracturing flow-back fluid were analysed. Simultaneously, the influence of current, electrolysis time and electrode plate spacing on H_2 production was investigated. This study aims to serve as a reference for the analysis of the H_2 evolution regular pattern in treating oilfield fracturing flow-back fluid using the electrochemical method.

2. Materials and Methods

2.1. Materials

The experimental fracturing flow-back fluid was obtained from the storage pool of fracturing flow-back liquid in Guangyuan oil

Received February 14, 2018 **Accepted** November 14, 2018

† Corresponding author
Email: ccww91@126.com, zhumijia128@163.com
Tel: +86-716-8060472 Fax: +86-716-8060472
ORCID: 0000-0003-0061-8305 (M. Zhu)

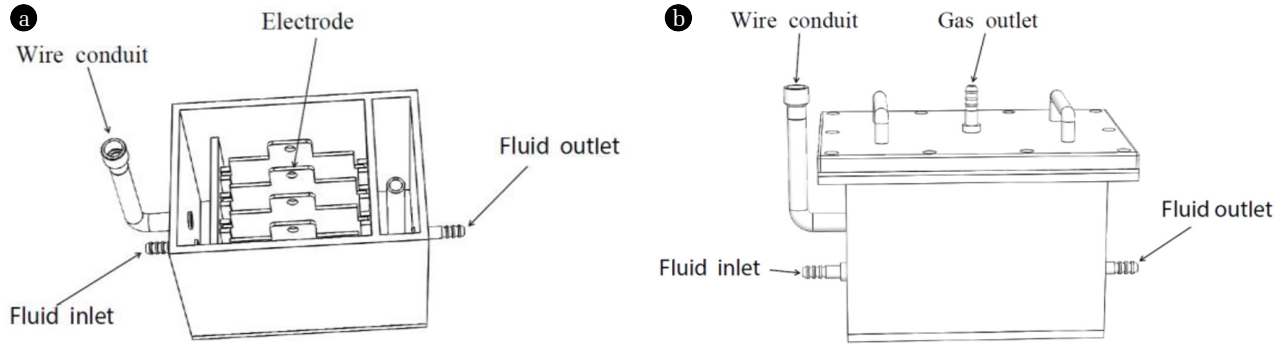

Fig. 1. Electrolysis treatment unit ((a): internal diagram; (b): external diagram).

and gas field of PetroChina. The electrode materials in the study included aluminium electrode (Al), titanium electrode (Ti), zirconium electrode (Zr), special ruthenium and iridium composite coating electrode (Ti/RuO_2-IrO_2, adapt to neutral and acid environment), ruthenium and iridium composite coating electrode (Ti/RuO_2-IrO_2, adapt to basic environment), special ruthenium and iridium palladium composite coating electrode (Ti/RuO_2-IrO_2-PdO, adapt to neutral and acid environment) and ruthenium and iridium palladium composite coating electrode (Ti/RuO_2-IrO_2-PdO, adapt to basic environment). The standard dimension was 100 mm × 90 mm × 3 mm. The electrode materials were produced by Baoji Longsheng non-ferrous Pioneer Metals Company (China). Electrolytic tank was used for the collection of gas from waste liquid through electrochemical treatment. The main components of the electrolytic tank included electrolysis, buffer and overflow rooms (showed in Fig. 1). The dimensions of the electrolysis, buffer, and overflow rooms were 120 mm × 144 mm × 105 mm (Total volume: 1,814.4 mL), 20 mm × 144 mm × 135 mm (Total volume: 388.8 mL) and 30 mm × 144 mm × 105 mm (Total volume: 583.2 mL), respectively. The tank was produced by the Feihong Plexiglass Products Company in Wuhan (China). DC regulated power supply type was XR (Shanghai Yize Electric Co., Ltd., China) (input voltage: 220 V + 10%, 50 Hz + 1 Hz; output voltage: 0-60 V; output current: 0-30 A).

2.2. Electrochemical Experiments

A total of 800 mL fracturing flow-back fluid from Guangyuan oil field was added to the electrolytic tank before the electrochemical process. Half of the electrodes were immersed in the solution, and the effective surface area of the electrode was 4,500 mm^2. The electrode material and electrode combination mode were changed, and the relationship among the H_2 production rate, energy consumption, decolourisation and turbidity removal rates of waste fluid in combination with different electrode materials was analysed. The parameters of electrochemical process, a direct current (DC) range of 0-2.5 A, an electrode plate spacing range of 2-10 cm and an electrolysis time range of 0-70 min were also examined. The batch experiments were conducted at room temperature (20℃).

2.3. Analysis Methods

The ion chromatograph ICS-2100 was from Thermo Fisher Scientific Co. Ltd. The electronic microbalance type was Sartorius BP211D (Switzerland) with a precision of 0.01 mg. The multifunction complex gas analyser was GT-2000 (Shenzhen city Kolno Electronic Technology Co., Ltd., China) with 1% - 3% precision. The gas mass flowmetre and cumulant indicator type was MFM610-RS232 (Suzhou Aituo Electronic Equipment Co., Ltd., China) with a range of 0-300 mL/min.

The colourity of the solutions described by Zeng et al. [16] was performed on a 751-GW UV/vis spectrophotometer (Inesa analytical instrument Co., Ltd., Shanghai, China). The maximum absorption wavelength at 339 nm was obtained by determining the colourity values. Standard solution samples were prepared from a commercial concentrated platinum cobalt colour solution. The samples were used for instrument calibration and for the development of a standard curve of colour and absorbance. The R^2 value associated with this curve was 0.9999. Colourity removal performance was calculated with the following equation: $R\% = [(A_0-A)/A_0] \times 100$. The turbidity metre was Orion AQ2010 (Thermo Electron Corporation).

The mechanism of gas production in electrolysis was analysed by means of oxygen evolution potential, chloride evolution potential and polarization curve. The oxygen evolution potential of electrode in 0.5 mol/L sulphate water solution, the chlorine evolution potential of electrode in saturated NaCl aqueous solution and the Tafel polarization curve of electrode in fracturing flow-back fluid sample were obtained on the CS350H electrochemical workstation (Wuhan Corrtest Instruments Co., Ltd., China).

3. Results and Discussion

3.1. Effect of Electrode Materials on H_2 Production

When the Ti, Al and Ti/RuO_2-IrO_2-PdO were used as anode, Al, Ti, Zr, Ti/RuO_2-IrO_2 and special Ti/RuO_2-IrO_2, Ti/RuO_2-IrO_2-PdO and special Ti/RuO_2-IrO_2-PdO were used as cathode, respectively. Results of H_2 gas production in the electrochemical process are described in Table 1.

Table 1 shows that when the cathode material was soluble aluminium electrode, the H_2 production (V_a) of the electrode combination was the largest, reaching 36.00, 45.85 and 45.98 mL. When the cathode material was a special Ti/RuO_2-IrO_2-PdO inert

Table 1. Effect of Electrode Materials on H_2 Production

Serial number	Cathode	Anode	H_2 production/mL
1		Ti/RuO_2-IrO_2-PdO	36.00
2	Al	Ti	45.85
3		Al	45.98
4		Ti/RuO_2-IrO_2-PdO	28.57
5	Ti	Ti	38.85
6		Al	45.87
7		Ti/RuO_2-IrO_2-PdO	25.02
8	Zr	Ti	34.83
9		Al	41.64
10		Ti/RuO_2-IrO_2-PdO	24.87
11	Special Ti/RuO_2-IrO_2	Ti	37.31
12		Al	42.90
13		Ti/RuO_2-IrO_2-PdO	25.89
14	Ti/RuO_2-IrO_2	Ti	38.63
15		Al	43.83
16		Ti/RuO_2-IrO_2-PdO	19.94
17	Special Ti/RuO_2-IrO_2-PdO	Ti	34.29
18		Al	38.87
19		Ti/RuO_2-IrO_2-0PdO	27.68
20	Ti/RuO_2-IrO_2-PdO	Ti	37.93
21		Al	41.76

electrode, the H_2 production (V_s) of the electrode combination was the lowest at 19.94, 34.29 and 38.87 mL. These results were equivalent to 55.39%, 74.78% and 84.54% of the H_2 production (V_s/V_a) when the cathode material was aluminium electrode. Different electrode materials considerably influenced H_2 production. H_2 production was low when the anode and cathode materials were both inert electrodes (however, H_2 production of different inert electrode combinations were different) due to the high potential inert electrode of H_2 and O_2. A high O_2 potential can lead to Cl_2 production of the anode. Apart from H_2 production, electron consumption of ClO^- led to the reduction of H_2 production when the current and electrolysis time were the same and the inert electrode was used as cathode [17-19].

3.2. Relationship between H_2 Production and Electrochemical Treatment Efficiency

The effect of different types of electrode combination on the colourity and turbidity removal rate in fracturing flow-back fluid treatment is shown in Table 2, where the range of turbidity removal and decolourisation rates were 54.26% - 62.77% and 37.92% - 39.75%, respectively, when Ti/RuO_2-IrO_2-PdO was used as an anode. When Al was used as an anode, the range of the turbidity removal and decolourisation rates reached 98.37% - 98.74% and 85.67% - 87.82%, respectively. Table 1 shows that when the cathode material of the electrode was the same and when the Ti/RuO_2-IrO_2-PdO, Ti and Al were used as anode, H_2 production increased, showing that H_2 production is related to the turbidity removal and decolourisation rates of the fracturing flow-back fluid in the Guangyuan oilfield.

H_2 production resulted in high turbidity removal and decolourisation rates in the treatment of the fracturing flow-back fluid. Al anode yielded the highest H_2 (45.98 mL) and resulted in the highest turbidity removal and decolourisation rate (98.74% and 87.82%, respectively). By contrast, the Ti/RuO_2-IrO_2-PdO anode and special Ti/RuO_2-IrO_2-PdO cathode produced 19.94 mL of H_2, with turbidity removal and decolourisation rate of 54.26% and 38.03%, respectively. When the current and electrolysis time were the same, the electrode combination, which produces considerable amount of H_2, usually exerts a satisfactory treatment effect. However, the safety of the electrolysis process must be considered because of the large production capacity of H_2.

3.3. Relationship between H_2 Production and Energy Consumption

The effect of different types of electrode combinations on the colourity and turbidity removal rate from fracturing flow-back fluid treatment is shown in Table 2. The energy consumption assessments of fracturing flow-back fluid treatment under different types of electrode combination are shown in Table 3.

Table 3 shows that when Al, Ti/RuO_2-IrO_2-PdO, Ti was used as anode, the energy consumption range of the electrode combinations was 26-28, 26-30 and 34-36 W·h, respectively. From Table 1-3, electricity consumption increased with the increase of H_2 production, turbidity removal and decolourisation rate. However, the comparative analysis results in Table 1 and 2 show that when Al was used as the anode, H_2 production, turbidity removal and decolourisation rate of the electrode combinations was high,

Table 2. Effect of Electrode Materials on Turbility Removal Rate and Decolourisation Rate

Serial number	Cathode	Anode	Turbidity removal rate/%	Decolourisation rate/%
1		Ti/RuO_2-IrO_2-PdO	57.45	39.75
2	Al	Ti	97.12	87.22
3		Al	98.74	87.82
4		Ti/RuO_2-IrO_2-PdO	60.64	38.74
5	Ti	Ti	95.32	86.12
6		Al	98.38	86.45
7		Ti/RuO_2-IrO_2-PdO	62.77	38.22
8	Zr	Ti	95.50	85.92
9		Al	98.56	87.01
10		Ti/RuO_2-IrO_2-PdO	57.45	38.13
11	Special Ti/RuO_2-IrO_2	Ti	94.95	84.27
12		Al	98.55	85.75
13		Ti/RuO_2-IrO_2-PdO	58.51	37.92
14	Ti/RuO_2-IrO_2	Ti	95.32	86.05
15		Al	98.37	86.27
16		Ti/RuO_2-IrO_2-PdO	54.26	38.03
17	Special Ti/RuO_2-IrO_2-PdO	Ti	95.14	87.05
18		Al	98.72	86.92
19		Ti/RuO_2-IrO_2-PdO	58.51	38.72
20	Ti/RuO_2-IrO_2-PdO	Ti	95.32	85.75
21		Al	98.38	85.67

Table 3. Effect of Electrode Materials on Energy Consumption

Serial number	Cathode	Anode	Energy consumption/W•h
1		Ti/RuO_2-IrO_2-PdO	30.00
2	Al	Ti	34.00
3		Al	26.00
4		Ti/RuO_2-IrO_2-PdO	26.00
5	Ti	Ti	34.00
6		Al	27.00
7		Ti/RuO_2-IrO_2-PdO	27.00
8	Zr	Ti	36.00
9		Al	27.00
10		Ti/RuO_2-IrO_2-PdO	28.00
11	Special Ti/RuO_2-IrO_2	Ti	36.00
12		Al	27.00
13		Ti/RuO_2-IrO_2-PdO	29.00
14	Ti/RuO_2-IrO_2	Ti	36.00
15		Al	28.00
16		Ti/RuO_2-IrO_2-PdO	29.00
17	Special Ti/RuO_2-IrO_2-PdO	Ti	35.00
18		Al	26.00
19		Ti/RuO_2-IrO_2-PdO	29.00
20	Ti/RuO_2-IrO_2-PdO	Ti	35.00
21		Al	27.00

although their energy consumption was low. These findings may be attributed to the soluble Al electrode. Al electrode was not only rapidly dissolved but also generated the flocculation effect of aluminium hydroxide flocs. The various pollutants in the form of floc sedimentation, which resulted in the consumption of the same electric energy, significantly increased turbidity removal and decolourisation rate [20, 21]. This finding may be due to the relatively low H_2 potential of the Al electrode, which resulted in an increase in the current efficiency during the electrochemical treatment, thereby reducing the energy consumption and causing H_2 evolution [17-19].

3.4. Effect of Different Electrolysis Condition on H_2 Production of Al(+)-Al(−) Electrode Combination

Table 1 shows that when Al(+)-Al(−) electrode combination was used in the fracturing flow-back fluid treatment, H_2 production was the largest under the same electrolysis conditions. Therefore, the Al(+)-Al(−) electrode combination was selected as a sample, the effect of electrolysis time, electrolysis current and electrode plate spacing on the H_2 production were shown in Fig. 2-4.

Fig. 2 shows that H_2 production from the electrode combination linearly increased with prolonged electrolysis under the same electrolysis conditions when the Al(+)-Al(−) electrode combination was used. This finding indicates that the electrochemical reactor uses the Al(+)-Al(−) electrode combination for a long time for waste fluid treatment. H_2 production linearly increased, and the risk due to H_2 also increased.

Fig. 3 shows that with the combination of Al(+)-Al(−) electrode, H_2 production from the electrode combination increases with increasing electrolysis current under the same electrolysis conditions. The increase rate also rises with increasing of electrolysis current. Increasing the electrolysis current was clearly beneficial to the production of H_2 from the Al(+)-Al(−) electrode combination. The main reactions occurring at the anode and cathode are as follows:

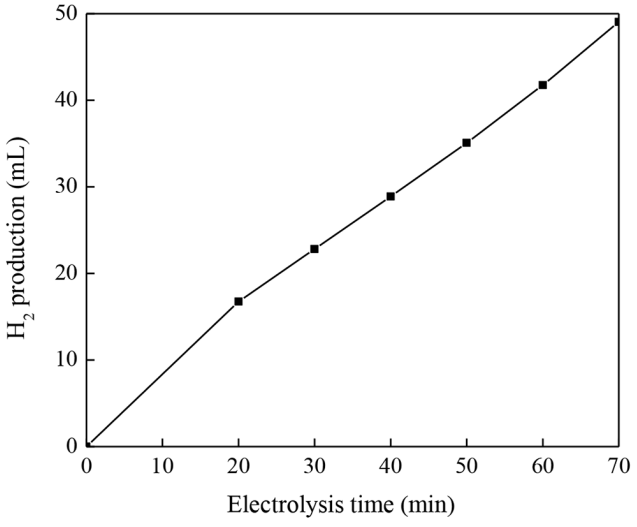

Fig. 2. H_2 production of Al(+)-Al(−) electrode combinations at different electrolysis times.

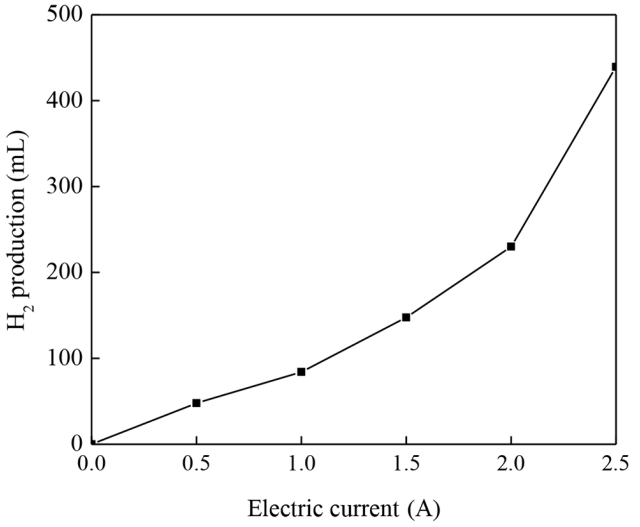

Fig. 3. H_2 production of Al(+)-Al(−) electrode combinations at different electric currents.

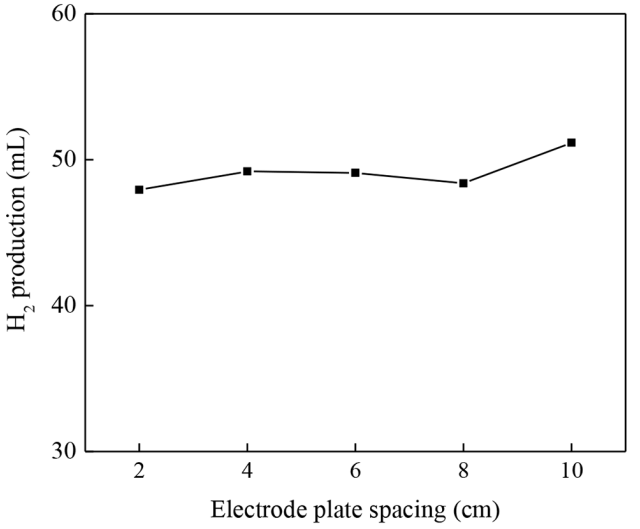

Fig. 4. H_2 production of Al(+)-Al(−) electrode combinations at different electrode plate spacings.

Anodic reaction:

$$Al - 3e \rightarrow Al^{3+} \quad (1)$$

Cathodic reaction:

$$2H^+ + 2e \rightarrow H_2\uparrow \quad (2)$$

Combination of the preceding analysis showed that a large H_2 production was conducive to improving the turbidity removal and decolourisation rate of fracturing flow-back fluid by electrochemical treatment.

As shown in Fig. 4, no evident change was observed in the gas evolution of H_2 between the Al(+)-Al(−) electrode combinations with the increase in electrode plate spacing. This observation can be attributed to the Guangyuan oilfield fracturing flow-back

fluid containing numerous ions, such as Cl^- and Na^+ (initial concentration: Na^+ 1,700 mg/L; Cl^- 7,000 mg/L, the change of concentration was not obvious after electrochemical treatment), thereby the fluid has excellent conductivity (19,000 μs/cm). Thus, increasing the electrode plate spacing will not significantly reduce the current efficiency.

3.5. Analysis of the Electrode Self-corrosion Potential, O_2 Evolution and Cl_2 Evolution Polarization Curve

Tafel electrode polarization curves of the Al electrode and special Ti/RuO_2-IrO_2-PdO are shown in Fig. 5(a) and (b), where the self-corrosion potentials of Al electrode and special Ti/RuO_2-IrO_2-PdO were −0.58 and 0.54 V, respectively. The self-corrosion potential of the Al electrode, which was an active metal electrode, was extremely low. Thus, the Al electrode formed Al^{3+} due to the easy occurrence of electron loss in the electrolysis anode reaction. However, the special Ti/RuO_2-IrO_2-PdO had a high self-corrosion potential and was an inert electrode. During the electrolysis anode reaction, the electrode could not easily lose electrons. OH^- or Cl^- adsorbed on the electrode was relatively more likely to lose electrons, thereby producing O_2 or Cl_2.

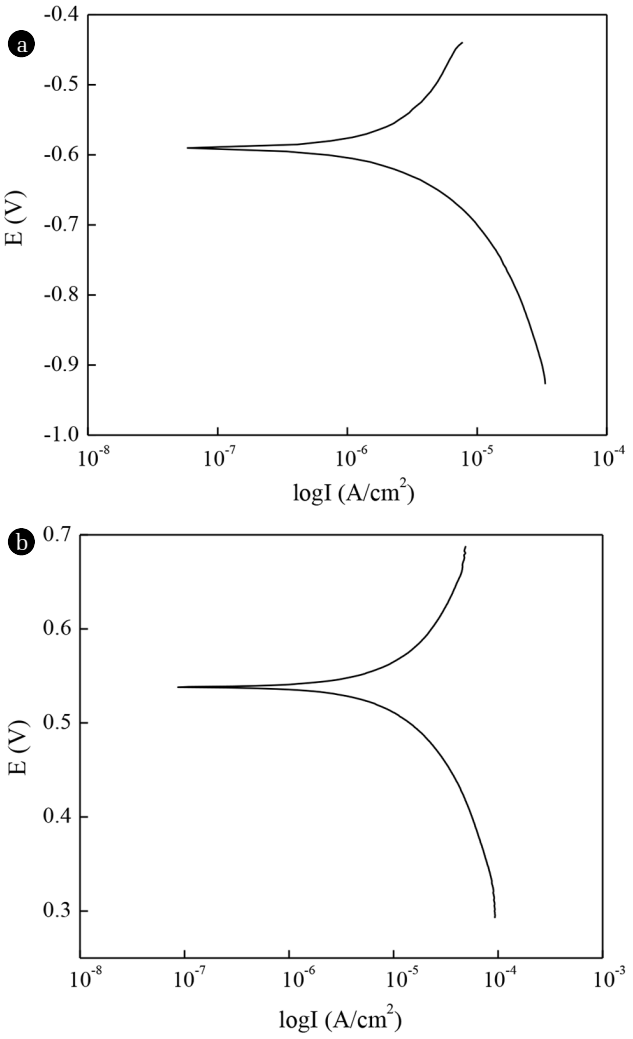

Fig. 5. The Tafel electrode polarization curves of Al electrode (a) and special Ti/RuO_2-IrO_2-PdO (b).

In the case of an inert electrode, the self-corrosion potentials of different coated electrodes were also different, as shown in Table 4.

Table 4 shows that the self-corrosion potential of the special Ti/RuO_2-IrO_2-PdO in the fracturing fluid in Guangyuan oilfield was the highest, whereas the self-corrosion potential of zirconium electrode was the lowest. Generally, when the self-corrosion potential was high, the electrode was inert. Therefore, the inert electrodes in Table 4 were sorted according to their inertness during the electrolysis treatment of fracturing flow-back fluid in Guangyuan oilfield as follows: Special Ti/RuO_2-IrO_2-PdO > Ti/RuO_2-IrO_2-PdO > Ti/RuO_2-IrO_2 > special Ti/RuO_2-IrO_2 > Ti > Zr.

Table 1 also shows that when the current and electrolysis time were the same and Ti/RuO_2-IrO_2-PdO was used as anode, H_2 production of each electrode combination was relatively low. However, the H_2 production at each electrode combination significantly increased when the Al electrode was used as the anode. The inert electrode may generate O_2 or Cl_2 because the Al electrode mainly formed Al^{3+} during the anode reaction. The generated gas type (O_2, Cl_2 or mixed gas of O_2 and Cl_2) of the inert electrode as an anode was clarified and its influence on H_2 production of different cathodes was determined. The inert electrode special Ti/RuO_2-IrO_2-PdO was used as an example to study the O_2 evolution and the Cl_2 evolution polarization curve as shown in Fig. 6(a) and (b), respectively.

Fig. 6(a) and (b) show that when special Ti/RuO_2-IrO_2-PdO was used as the anode, evolutions of the O_2 and Cl_2 potential were 1.17 and 1.24 V, respectively. Moreover, O_2 evolution potential was lower than the Cl_2 evolution potential, indicating that O_2 was easier to generate than Cl_2. Therefore, O_2 was mainly generated from the anode. However, the difference between O_2 evolution potential and Cl_2 evolution potential was only 0.07 V, indicating that the anode was also likely to generate Cl_2. The use of an inert electrode as an anode in the processing of fracturing flow-back fluid in Guangyuan oilfield resulted in the production of O_2 and Cl_2. Cl_2 can be dissolved in aqueous solution and forms HClO. After dissociation, it can form ClO^-, which can obtain electrons from the cathode, thereby reducing the H_2 production of the cathode. This finding also verified the results shown in Table 1.

Table 4. Self-corrosion Potentials of Different Cathode Materials

Serial number	Cathode material	Self-corrosion potentials/V
1	Ti	0.081
2	Zr	0.047
3	Special Ti/RuO_2-IrO_2	0.264
4	Ti/RuO_2-IrO_2	0.275
5	Special Ti/RuO_2-IrO_2-PdO	0.540
6	Ti/RuO_2-IrO_2-PdO	0.284

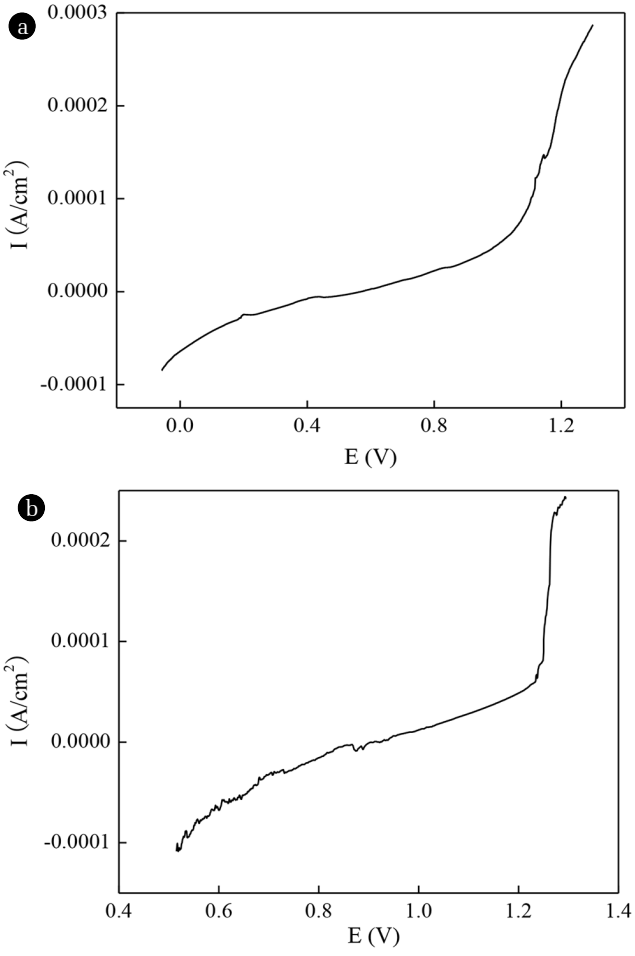

Fig. 6. The oxygen evolution polarization curve (a) and chloride evolution polarization curve (b) of a special Ti/RuO_2-IrO_2-PdO as an anode.

Therefore, the reaction mechanism of inert electrode in Table 1 was speculated as follows:

Anodic reaction:

$$H_2O - 2e \rightarrow O_2\uparrow + 2H^+ \quad (3)$$

$$2Cl^- - 2e \rightarrow Cl_2\uparrow \quad (4)$$

$$Cl_2 + H_2O \rightarrow ClO^- + 2H^+ + Cl^- \quad (5)$$

Cathodic reaction:

$$ClO^- + H_2O + 2e \rightarrow 2Cl^- + 2OH^- \quad (6)$$

4. Conclusions

i) The combination of electrode material and electrode significantly affected H_2 evolution. When the anode and cathode materials were both inert electrodes, H_2 production was low, and the anode material was a soluble Al electrode; therefore, H_2 production was high.

ii) A large amount of H_2 led to the high turbidity removal and decolourisation rate of the electrode combination was used for the treatment of fracturing flow-back fluid in the Guangyuan oilfield.

iii) Under the same current and electrolysis time, the energy consumption of cathodic material using soluble Al electrode was lower than that of the inert electrode.

iv) The turbidity removal and decolourisation rate of fracturing flow-back fluid were highest using Al(+)-Al(−) electrode combination. Prolonged electrolysis time and increasing the current can significantly enhance H_2 production, especially, electrolysis current played an important role in H_2 production.

v) When inert electrode was used as an anode for the treatment of fracturing flow-back fluid in Guangyuan oilfield, the main anodic gases were O_2 and Cl_2, Cl_2 can be dissolved in aqueous solution to form ClO^- after dissociation. The dissolution reduces the amount of H_2 produced by the cathode.

Acknowledgments

The authors of this work wish to gratefully acknowledge the financial support from The Key Technologies R&D Program of China (No.2016ZX05040003-008-001).

References

1. Zhang F, Shen Y, Wang L, Ma G, Su Y, Ren T. Synthesis and properties of polyacrylamide drag reducer for fracturing fluid. *Chem. Ind. Eng. Prog.* 2016;33:3640-3644 (in Chinese).
2. Ye D, Wang S, Cai Y, Ren Y, Luo C. Application of continuously mixing fracturing fluid and such flow process. *Nat. Gas Ind.* 2013;33:47-51 (in Chinese).
3. Yang Z, Wei Y, Lu L, Zhang S, Wang Z. Research and application of recycling treatment technology for shale gas fracturing flowback fluid: A case study. *Nat. Gas Ind.* 2015;35:131-137 (in Chinese).
4. Valero E, Álvarez X, Cancela Á, Sánchez Á. Harvesting green algae from eutrophic reservoir by electroflocculation and post-use for biodiesel production. *Bioresour. Technol.* 2015; 187:255-262.
5. Moheimani NR, Tetraselmis S. Culture for CO_2 bioremediation of untreated flue gas from a coal-fired power station. *J. Appl. Phycol.* 2016;28:2139-2146.
6. Vivek JP, Burgess IJ. Insight into chloride induced aggregation of DMAP-monolayer protected gold nanoparticles using the thermodynamics of ideally polarized electrodes. *J. Phys. Chem. C* 2016;112:2872-2880.
7. Gómez-López VM, Gil MI, Pupunat L, Allende A. Cross-contamination of *Escherichia coli* O157:H7 is inhibited by electrolyzed water combined with salt under dynamic conditions of increasing organic matter. *Food Microbiol.* 2015;46:471-478.
8. Tanneru CT, Rimer JD, Chellam S. Sweep flocculation and adsorption of viruses on aluminum flocs during electro-

chemical treatment prior to surface water microfiltration. *Environ. Sci. Technol*. 2013;47:4612-4618.
9. Zhao W, Zhu H, Zong Z, Xia J, Wei X. Electrochemical reduction of pyrite in aqueous NaCl solution. *Fuel* 2005;84:235-238.
10. Sánchez J, Butter B, Rivas BL, Basáez L, Santander P. Electrochemical oxidation and removal of arsenic using water-soluble polymers. *J. Appl. Electrochem*. 2015;45:151-159.
11. Sopaj F, Rodrigo MA, Oturan N, Podvorica FI, Pinson J, Oturan MA. Influence of the anode materials on the electrochemical oxidation efficiency. Application to oxidative degradation of the pharmaceutical amoxicillin. *Chem. Eng. J.* 2015;262: 286-294.
12. Alvarezpugliese CE, Morenowiedman P, Machucamartínez F, Marriagacabrales N. Distillery wastewater treated by electrochemical oxidation with boron-doped diamond electrodes. *J. Adv. Oxid. Technol*. 2016;14:213-219.
13. Geng Z, Wang X, Guo X, Zhang Z, Chen Y, Wang Y. Electrodeposition of chitosan based on coordination with metal ions *in situ*-generated by electrochemical oxidation. *J. Mater. Chem. B* 2016;4:3331-3338.
14. Chen WF, Muckerman JT, Fujita E. Recent developments in transition metal carbides and nitrides as hydrogen evolution electrocatalysts. *Chem. Commun*. 2013;49:8896-8909.
15. Ci SQ, Mao S, Hou Y, et al. Rational design of mesoporous NiFe-alloy-based hybrids for oxygen conversion electrocatalysis. *J. Mater. Chem. A* 2015;3:7986-7993.
16. Zeng F, Luo X. Determination of the colority of water samples by spectrophotometry. *Ind. Water Treat*. 2006;26:69-77 (in Chinese).
17. Jang SH, Lee JH. Fabrication of nickel cobalt oxide electrode by in situ electrochemical method for the oxygen evolution anodes in water electrolysis system. *J. Nanosci. Nanotechnol*. 2016;16:11326-11329.
18. Swesi AT, Masud J, Nath M. Nickel selenide as a high-efficiency catalyst for oxygen evolution reaction. *Energ. Environ. Sci.* 2016;9:1771-1782.
19. Schaefer H, Sadaf S, Walder L, et al. Stainless steel made to rust: A robust water-splitting catalyst with benchmark characteristics. *Energ. Environ. Sci*. 2015;8:2685-2697.
20. Mouedhen G, Feki M, Wery MP, Ayedi HF. Behavior of aluminum electrodes in electrocoagulation process. *J. Hazard. Mater*. 2008;150:124-135.
21. Pournaghi-Azar MH, Razmi-Nerbin H. Electroless preparation and electrochemistry of nickel-pentacyanonitrosylferrate film modified aluminum electrode. *Electroanalysis* 2015;12:209-215.